Letters

A Novel Clamp Coil Assisted IPT Battery Charger With Inherent CC-to-CV Transition Capability

Zhicong Huang, *Member, IEEE*, Guoyu Wang, Jidong Yu, and Xiaohui Qu, *Senior Member, IEEE*

***Abstract*—A constant current (CC) output followed by a constant voltage (CV) threshold is usually needed for an inductive power transfer (IPT) charger to comply with the battery charging profile. This letter proposes a novel clamp coil assisted IPT battery charger that features inherent, passive, automatic, and smooth CC-to-CV transition. Since the CC-to-CV transition eliminates the necessity of state-of-charge detection, wireless feedback communication, and active control, the proposed IPT charger is rugged and reliable. The inherent CC-to-CV transition capability also tackles the open-circuit risk during a CC charging process. As minimalist design is achieved in the secondary, the proposed IPT charger is suitable for wireless onboard charging applications. Near-unity power factor design is also considered to minimize the voltage–ampere rating and permits soft switching. Experiment results validate the inherent CC-to-CV transition capability.**

***Index Terms*—Battery charging, constant current (CC), constant voltage (CV), inductive power transfer (IPT), passive solution.**

I. Introduction

CURRENTLY, inductive power transfer (IPT) technologies can pass energy efficiently via the magnetic field coupling [1]. Without the physical contact, IPT shows significant benefits in providing user-friendly and maintenance-free operations in battery charging applications. The widely used high-power-density Li-ion battery is generally charged at a constant current (CC). Once the CC charging is near completion, a constant voltage (CV) threshold usually follows to fully charge the battery and protect the battery from overvoltage damage [2]. Therefore, to comply with the charging profile, an IPT battery charger desires a CC output as well as a CV threshold, as shown by Fig. 1.

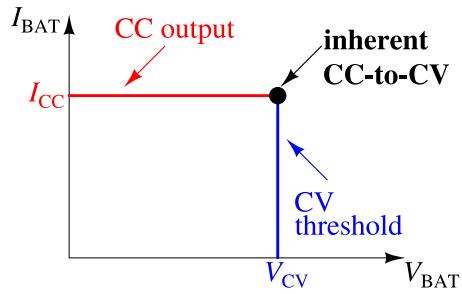

Fig. 1. Desired output V–I characteristics for IPT battery chargers.

To realize the CC-to-CV transition, it is an intuitive idea to cascade an additional dc/dc converter at the secondary side of the IPT converter to regulate the required CC output and CV threshold [3]. Although control design in the primary can be eliminated, the penalties are the additional converter stage and corresponding control, which increase the power losses and cost. Keeping a single-stage design in mind, load-independent-current (LIC) and -voltage (LIV) transfer characteristics of IPT converters have been widely studied and applied for the CC output and CV threshold, respectively, [4]–[8]. In [4]–[6], an IPT converter can be designed with a single compensation topology and hops its operating frequency from the LIC point to the LIV point. Alternatively, to keep the operating frequency fixed, hybrid compensation topologies can be designed and switched by several bidirectional switches for the transition from the LIC mode to the LIV mode [7], [8]. Although the abovementioned LIC- and LIV-based methods can simplify the output current or voltage control design, the battery state-of-charge (SOC) detection and wireless feedback communication are inevitable for the transition from a CC output to a CV threshold as not to damage the battery. Such schemes increase control circuit complexity and are less rugged.

This letter proposes a novel clamp coil assisted IPT battery charger that enables an automatic transition from the CC output to the CV threshold during the battery charging process. Such that, the proposed IPT charger features high robustness without battery SOC detection and wireless feedback communication. The proposed system adopts a basic series–series (SS) compensation topology in the primary and secondary to provide CC charging. The inherent CC-to-CV transition is achieved by a

Manuscript received November 18, 2020; revised December 28, 2020; accepted January 23, 2021. Date of publication January 26, 2021; date of current version May 5, 2021. This work was supported in part by the National Natural Science Foundation of China under Grants 52077038 and 52007067, in part by the Natural Science Foundation of Jiangsu Province under Grant BK20181280, and in part by the Fundamental Research Funds for Central Universities of China. *(Corresponding author: Xiaohui Qu.)*

Zhicong Huang is with the Shien-Ming Wu School of Intelligent Engineering, South China University of Technology, Guangzhou 510006, China (e-mail: zhiconghuang@scut.edu.cn).

Guoyu Wang, Jidong Yu, and Xiaohui Qu are with the School of Electrical Engineering, Southeast University, Nanjing 210096, China (e-mail: 522558305@qq.com; 1499446593@qq.com; xhqu@seu.edu.cn).

Color versions of one or more figures in this article are available at https://doi.org/10.1109/TPEL.2021.3054768.

Digital Object Identifier 10.1109/TPEL.2021.3054768

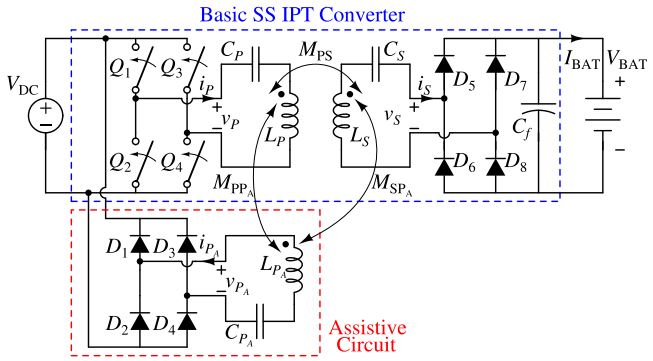

Fig. 2. Proposed clamp coil assisted IPT battery charger.

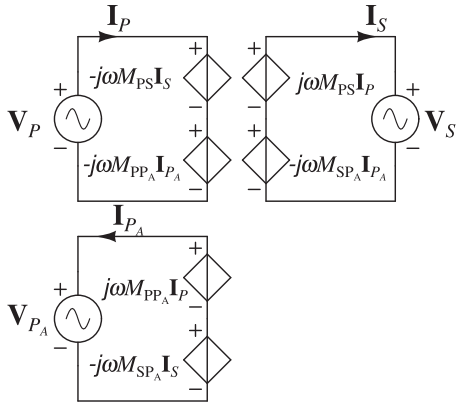

Fig. 3. Equivalent circuit of Fig. 2.

third coil clamping the primary resonant current, so as to limit the secondary induced output voltage to be within a specified threshold. Unlike a single SS IPT converter, the proposed clamp coil can also function as the open-circuit protection during CC charging. As minimalist design is achieved in the secondary, the proposed IPT charger is suitable for wireless onboard charging applications. Moreover, near-unity power factor for a minimum voltage–ampere rating is also considered to permit soft switching. Experiment results are presented to validate performances of the proposed IPT system.

II. Theoretical Analysis of Proposed Clamp Coil Assisted IPT Battery Charger

The proposed clamp coil assisted IPT battery charger is shown in Fig. 2, which can be regarded as the combination of a basic SS compensated IPT converter and a clamp coil based assistive circuit. The assistive circuit only includes a clamp coil, a compensation capacitor, and a diode rectifier, which is a passive, simple, control-free, and reliable solution. The loosely coupled transformer is, thus, formed of a primary coil, a clamp coil, and a secondary coil, whose self-inductances are denoted as L_P, L_{P_A}, and L_S, respectively.

From Fig. 2, v_P is chopped from input dc voltage $V_{\rm DC}$ via a full-bridge inverter $Q_{1,2,3,4}$, where v_{P_A} is rectified and filtered also as $V_{\rm DC}$ via a full-bridge diode rectifier $D_{1,2,3,4}$. $V_{\rm DC}$ can be modulated by $Q_{1,2,3,4}$ with D being the duty cycle of v_P half cycle. The fundamental component of the square voltage v_P, denoted as v_{P1}, is given as follows:

$$v_{P1}(t) = \frac{4V_{\rm DC}}{\pi} \sin\frac{\pi D}{2} \sin(\omega t + \theta). \tag{1}$$

If the assistive rectifier is fully conducted, the fundamental component of the square voltage v_{P_A}, denoted as v_{P_A1}, is also given as follows:

$$v_{P_A1}(t) = \frac{4V_{\rm DC}}{\pi} \sin(\omega t + \delta). \tag{2}$$

The phase angle between $v_{P1}(t)$ and $v_{P_A1}(t)$ is determined by phases of i_P and i_{P_A}.

Unless specify otherwise, subscripts P, P_A, and S indicate parameters in the primary, assistive, and secondary circuits, respectively. Then, mutual inductances among these three coils are defined as $M_{\rm PS}$, $M_{\rm PP_A}$, and $M_{\rm SP_A}$. Similar to [4]–[8], the mutual inductances should be considered as constant once the transformer is designed, and thus, the proposed system is most suitable for IPT charging applications that seldom have misalignment issues. C_P, C_{P_A}, and C_S are the series compensation capacitors, with which all the three coils are fully compensated at a fixed operating angular frequency ω. It gives

$$\omega = \frac{1}{\sqrt{L_P C_P}} = \frac{1}{\sqrt{L_{P_A} C_{P_A}}} = \frac{1}{\sqrt{L_S C_S}}. \tag{3}$$

A. Native Constant Current Output

Designed with (3), all the three resonance tanks have null reactances, and the equivalent circuit of Fig. 2 can be redrawn as Fig. 3. Here, $\mathbf{V}_P$, $\mathbf{V}_{P_A}$, $\mathbf{V}_S$, $\mathbf{I}_P$, $\mathbf{I}_{P_A}$, and $\mathbf{I}_S$ are vectors of fundamentals of v_P, v_{P_A}, v_S, i_P, i_{P_A}, and i_S, respectively. R_E is defined as the equivalent load of a secondary diode rectifier $D_{5,6,7,8}$ and battery load R_L. And, $R_E = \frac{8}{\pi^2} R_L$, where $R_L = \frac{V_{\rm BAT}}{I_{\rm BAT}}$. From Fig. 3, we have

$$\mathbf{V}_P = -j\omega M_{\rm PS}\mathbf{I}_S - j\omega M_{\rm PP_A}\mathbf{I}_{P_A} \tag{4}$$

$$\mathbf{V}_S = R_E\mathbf{I}_S = j\omega M_{\rm PS}\mathbf{I}_P - j\omega M_{\rm SP_A}\mathbf{I}_{P_A} \tag{5}$$

$$\mathbf{V}_{P_A} = j\omega M_{\rm PP_A}\mathbf{I}_P - j\omega M_{\rm SP_A}\mathbf{I}_S. \tag{6}$$

At the beginning of charging, R_L is small. By (5) and (6), the primary current $\mathbf{I}_P$ is not so large that the amplitude of $\mathbf{V}_{P_A}$ cannot exceed the input bus voltage $V_{\rm DC}$, as follows:

$$|\mathbf{V}_{P_A}| \le V_{\rm DC} \tag{7}$$

where $D_{5,6,7,8}$ are reverse biased, and $i_{P_A} = 0$.

The proposed IPT charger starts working with deactivation of the assistive circuit, and it operates as a conventional SS IPT converter [4]. With (4) and (5), a CC secondary output can be achieved as follows:

$$\mathbf{I}_S = -\frac{\mathbf{V}_P}{j\omega M_{\rm PS}}. \tag{8}$$

Moreover, since the reflected impedance from the secondary to the primary will be purely resistive, an input zero-phase angle (ZPA) can be achieved.

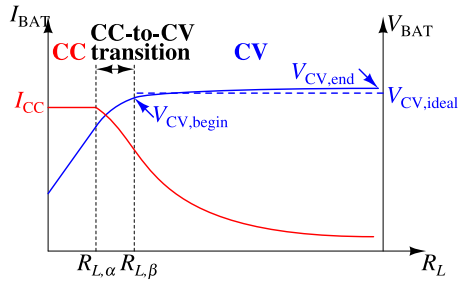

Fig. 4. Diagram of practical charging profile.

Although i_{P_A} is zero in the assistive circuit, the nearly sinusoidal induced voltage v_{P_A} in the clamp coil is not zero. Using (1) and (6), $|\mathbf{V}_{P_A}|$ increases with R_L, given as follows:

$$|\mathbf{V}_{P_A}| = \frac{4V_{\mathrm{DC}}}{\pi}\sin\frac{\pi D}{2}\sqrt{\left(\frac{M_{\mathrm{PP_A}}}{M_{\mathrm{PS}}}\frac{\frac{8}{\pi^2}R_L}{\omega M_{\mathrm{PS}}}\right)^2+\left(\frac{M_{\mathrm{SP_A}}}{M_{\mathrm{PS}}}\right)^2}. \tag{9}$$

Once $|\mathbf{V}_{P_A}|$ reaches V_{DC}, the assistive diode rectifier begins to be activated and the CC charging will not be maintained. The criterion for deactivation of the assistive circuit given in (7) yields the first transition point $R_{L,\alpha}$, as shown in Fig. 4

$$R_{L,\alpha} = \frac{\pi^2\omega M_{\mathrm{PS}}^2}{8M_{\mathrm{PP_A}}}\sqrt{\frac{\pi^2}{16\sin^2\frac{\pi D}{2}}-\left(\frac{M_{\mathrm{SP_A}}}{M_{\mathrm{PS}}}\right)^2}. \tag{10}$$

With (8) and (10), a CC output can be highlighted as follows:

$$I_{\mathrm{CC}} = \frac{8}{\pi^2}\frac{V_{\mathrm{DC}}}{\omega M_{\mathrm{PS}}},\ \text{for}\ R_L \le R_{L,\alpha}. \tag{11}$$

B. Transition Process

When $R_L > R_{L,\alpha}$, the assistive circuit comes to activation with the increasing R_L, and the CC charging process terminates. $v_{P_A}(t)$ is not a sinusoidal wave with its peak range clamped to V_{DC}. When $D_{5,6,7,8}$ are fully conducted, v_{P_A} is clamped to be a square wave, with its fundamental component subjecting to (2), i.e.,

$$|\mathbf{V}_{P_A}| = \frac{4}{\pi}V_{\mathrm{DC}}. \tag{12}$$

Thus, if $V_{\mathrm{DC}} < |\mathbf{V}_{P_A}| < \frac{4}{\pi}V_{\mathrm{DC}}$, the assistive rectifier keeps partially conducted with a discontinuous current i_{P_A}. The discontinuous current can be assumed to be very small, i.e., $i_{P_A} \approx 0$. Then, the criterion for full activation of the assistive rectifier given in (12) yields the second changeover point $R_{L,\beta}$, as shown in Fig. 4

$$R_{L,\beta} = \frac{\pi^2\omega M_{\mathrm{PS}}^2}{8M_{\mathrm{PP_A}}}\sqrt{\frac{1}{\sin^2\frac{\pi D}{2}}-\left(\frac{M_{\mathrm{SP_A}}}{M_{\mathrm{PS}}}\right)^2}. \tag{13}$$

When $R_L > R_{L,\beta}$, the assistive rectifier is fully activated.

There exists a transition process for $R_L \in (R_{L,\alpha}, R_{L,\beta}]$ with a partially conducted assistive rectifier. Comparing (10) and (13), the transition process locates in a short load range. As the IPT charger can go into CV charging at $R_L > R_{L,\beta}$, the required CC and CV outputs for most load ranges can be ensured.

C. Self-Sustained Constant Voltage Threshold

When $R_L > R_{L,\beta}$, a self-sustained CV output is required, i.e., $|\mathbf{V}_S|$ is required constant. Now, the assistive diode rectifier is fully conducted, $|\mathbf{V}_{P_A}| \equiv \frac{4V_{\mathrm{DC}}}{\pi}$. Also, $|\mathbf{V}_P| = \frac{4V_{\mathrm{DC}}}{\pi}\sin\frac{\pi D}{2}$. With constant $|\mathbf{V}_P|$, $|\mathbf{V}_S|$, and $|\mathbf{V}_{P_A}|$ for different R_L in (4), (5), and (6), the only solution is to make $M_{\mathrm{SP_A}} = 0$, such that $|\mathbf{I}_P|$ is clamped to a constant amplitude. Then, the output voltage induced from the clamped i_P is constant as follows:

$$V_{\mathrm{CV,ideal}} = \frac{\pi}{4}|\mathbf{V}_S| = \frac{M_{\mathrm{PS}}}{M_{\mathrm{PP_A}}}V_{\mathrm{DC}},\ \text{for}\ R_L > R_{L,\beta}. \tag{14}$$

Ideally, if $M_{\mathrm{SP_A}}$ is designed to be negligible, the proposed IPT system has a self-sustained CV threshold $V_{\mathrm{CV,ideal}}$ when $R_L > R_{L,\beta}$, as indicated in Fig. 4.

In the practical design, the assistive coil and the primary coil are usually coaxial in the primary side. $V_{\mathrm{CV,ideal}}$ can be readily adjusted by designing the assistive coil winding, i.e., $M_{\mathrm{PP_A}}$. Due to the relatively large gap distance, $M_{\mathrm{SP_A}}$ is relatively small. Nevertheless, practical effect of $M_{\mathrm{SP_A}}$ on the voltage output should be taken into consideration by separately analyzing the IPT charger in the following two situations.

1) If R_L is slightly larger than $R_{L,\beta}$, the assistive circuit begins to be activated. Compared with i_S that is still near its maximum value in the CC stage, i_{P_A} is very small. Thus, the insignificant i_{P_A} can be approximated as zero. Substituting (13) into (4) and (5), the output voltage at $R_{L,\beta}$ can be derived as follows:

$$\begin{aligned} V_{\mathrm{CV,begin}} &= \frac{\pi}{4}|\mathbf{V}_S| \\ &= \frac{M_{\mathrm{PS}}}{M_{\mathrm{PP_A}}}V_{\mathrm{DC}}\sqrt{1-\left(\frac{M_{\mathrm{SP_A}}}{M_{\mathrm{PS}}}\right)^2\sin^2\frac{\pi D}{2}}. \end{aligned} \tag{15}$$

2) If R_L increase far from $R_{L,\beta}$, i_S becomes insignificant and, thus, can be approximated as zero. For the assistive rectifier, the conducting current $|\mathbf{I}_{P_A}|$ should be always in phase with $|\mathbf{V}_{P_A}|$. Thus, in (4) and (6), $|\mathbf{V}_{P_A}|$ leads $|\mathbf{V}_P|$ a phase of 90°, while $|\mathbf{I}_{P_A}|$ leads $|\mathbf{I}_P|$ a phase of 90°. With (5), the output voltage is constant as follows:

$$\begin{aligned} V_{\mathrm{CV,end}} &= \frac{\pi}{4}|\mathbf{V}_S| \\ &= \frac{M_{\mathrm{PS}}}{M_{\mathrm{PP_A}}}V_{\mathrm{DC}}\sqrt{1+\left(\frac{M_{\mathrm{SP_A}}}{M_{\mathrm{PS}}}\right)^2\sin^2\frac{\pi D}{2}}. \end{aligned} \tag{16}$$

By (15) to (16), with the effect of $M_{\mathrm{SP_A}}$, the output voltage v_{BAT} slightly varies from $V_{\mathrm{CV,begin}}$ to $V_{\mathrm{CV,end}}$ with R_L increasing from $R_{L,\beta}$ to infinity, as indicated in Fig. 4. Nevertheless, the self-sustained CV is insusceptible, because $V_{\mathrm{CV,begin}}$ and $V_{\mathrm{CV,end}}$ are close to $V_{\mathrm{CV,ideal}}$ given $M_{\mathrm{SP_A}} \ll M_{\mathrm{PS}}$.

Similar to the CC stage, since the reflected impedances from the secondary to the primary and from the assistive circuit to the primary are both approximately resistive, input ZPA can also

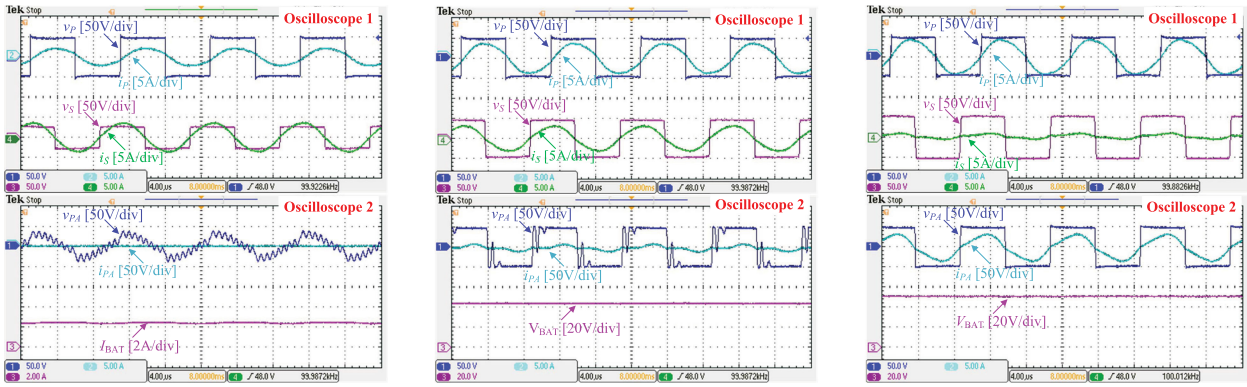

Fig. 5. Measured operating waveforms of the proposed system. (a) CC mode, $R_L = 10\,\Omega$. (b) Transition process, $R_L = 18\,\Omega$. (c) CV mode, $R_L = 100\,\Omega$.

TABLE I
MEASURED CIRCUIT PARAMETERS

Parameters	Values
L_P, L_{P_A}, L_S	99.4 μH, 43.4 μH, 82.26 μH
$M_{\rm PS}$, $M_{\rm PP_A}$, $M_{\rm SP_A}$	25.2 μH, 25.6 μH, 6.8 μH
C_P, C_{P_A}, C_S	26.2 nF, 59.9 nF, 29.47 nF
Models of Q_1–Q_4, D_1–D_8	IRF640, MBR20200

be achieved. A slight modulation of the input phase angle will facilitate the soft switching of $Q_{1,2,3,4}$.

It is known that the basic SS compensated IPT charger commonly has over-current risk in the primary if the battery load is accidentally open-circuit during the CC charging. However, in the same accidental open-circuit situation, there is no such problem for the proposed clamp coil assisted IPT charger, because $|\mathbf{I}_P|$ is clamped to a specified (safe) value immediately. Therefore, the proposed clamp coil not only enables the automatic CC-to-CV transition but also functions the open-circuit protection.

III. IMPLEMENTATION AND EXPERIMENTAL VERIFICATION

An experimental prototype is built with schematics shown in Fig. 2. The design of the three-coil loosely coupled transformer can be started with charging specifications of a battery. Given a battery with capacity of 10 Ah and nominal voltage of 48 V, the desired charging current and charging threshold voltage can be set at $I_{\rm CC} = 2.5$ A and $V_{\rm CV,end} = 52$ V, respectively. In general, two key steps can be carried out for the three-coil transformer design as follows. With (11) and the desired $I_{\rm CC}$, $M_{\rm PS}$ can be derived, such that the design can be started with the primary coil and the secondary coil. After that with (14) and the desired $V_{\rm CV,end}$, $M_{\rm PP_A}$ can be derived for designing the clamped coil. Detailed implementation of coil design with finite element analysis can refer to some existing iteration-based coil design methods, such as Bosshard *et al.* [10]. Measured circuit parameters are given in Table I. The operating frequency is fixed at 100 kHz. The proposed system is driven by a dc voltage source with $V_{\rm DC} = 48$ V, while the battery is emulated by an electronic load.

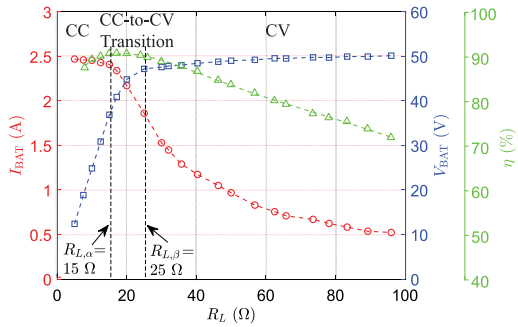

Fig. 6. Measured $I_{\rm BAT}$, $V_{\rm BAT}$, and η versus R_L.

With (10) and (13), the calculated $R_{L,\alpha}$ and $R_{L,\beta}$ are 14.2 Ω and 18.5 Ω, respectively. Thus, experimental waveforms at $R_L = 10\,\Omega$, $R_L = 18\,\Omega$, and $R_L = 100\,\Omega$ are captured for the CC mode, CC-to-CV transition, and CV mode, respectively, as shown in Fig. 5. Since there are seven signals in total, two four-channel oscilloscopes are used to capture the waveforms synchronously for a better demonstration. In the CC mode, as shown in Fig. 5(a), i_{P_A} is null and D_1–D_4 of the assistive rectifier are reverse biased, such that the system operates as a conventional SS IPT converter to achieve a CC output. During the CC-to-CV transition, as shown in Fig. 5(b), the assistive rectifier comes to early activation as D_1–D_4 are partly conducted. i_{P_A} is still small and thus in a discontinuous conduction mode. In the later CV mode, as shown in Fig. 5(c), due to the full activation of the assistive rectifier, i_P is being clamped for the achievement of a CV output. Moreover, there is no over-current problem in the primary even if the secondary is open circuit, i.e., R_L tends to be ∞. During the whole charging process, v_P always leads i_P a small phase angle, which permits the zero-voltage switching of Q_1–Q_4 and ensures low reactive power circulating in the circuit.

The measured $I_{\rm BAT}$ (marked with "◯") and $V_{\rm BAT}$ (marked with "□") versus R_L are plotted in Fig. 6. An approximate CC output at 2.5 A can be achieved when $R_L \le 15\ \Omega$, while an approximate CV threshold at 50 V is maintained if $R_L \ge 25\ \Omega$. It can be observed that, the practical $R_{L,\beta}$ (25 Ω) is slightly

larger than the calculated one (18.5 Ω). The deviation is caused by that i_{P_A} is still in a discontinuous current mode [9] in the early CV mode, and thus, fundamental approximation used in the theoretical analysis is not sufficiently precise. Nevertheless, the required inherent CC-to-CV transition can be achieved in a short load range. The measured η (marked with "△") versus R_L is also plotted in Fig. 6. A maximum efficiency of 90.2% is achieved at 18 Ω. In the CC stage, the assistive circuit is not activated ($i_{P_A} = 0$), no power losses are incurred in the assistive circuit. In the CC-to-CV transition process and early CV stage, due to $i_{P_A} \approx 0$, the efficiency is not affected too much by the power losses incurred by the assistive circuit. In the late CV stage (light load conditions), power losses incurred by the assistive circuit become significant as i_{P_A} increases with the decrease of output power. It is acceptable that penalty in efficiency caused by the use of the assistive circuit only occurs in the light load conditions.

IV. Conclusion

To achieve automatic and smooth CC to CV transition for battery charging, a novel clamp coil assisted IPT battery charger is proposed in this letter featuring inherent CC-to-CV transition. Thus, no SoC detection, wireless feedback communication or active control is needed. The design criteria and characteristics for each charging mode are derived in detail. Moreover, the inherent CC-to-CV transition capability also tackles the open-circuit risk during CC charging. Experiment results validate the theoretical analysis well.

References

[1] G. A. Covic and J. T. Boys, "Inductive power transfer," *Proc. IEEE*, vol. 101, no. 6, pp. 1276–1289, Jun. 2013.

[2] A. A. Hussein and I. Batarseh, "A review of charging algorithms for nickel and lithium battery chargers," *IEEE Trans. Veh. Technol.*, vol. 60, no. 3, pp. 830–838, Mar. 2011.

[3] Z. Li, C. Zhu, J. Jiang, K. Song, and G. Wei, "A 3-kW wireless power transfer system for sightseeing car supercapacitor charge," *IEEE Trans. Power Electron.*, vol. 32, no. 5, pp. 3301–3316, May 2017.

[4] Z. Huang, S. C. Wong, and C. K. Tse, "Design of a single-stage inductive-power-transfer converter for efficient EV battery charging," *IEEE Trans. Veh. Technol.*, vol. 66, no. 7, pp. 5808–5821, Jul. 2017.

[5] V. B. Vu, D. H. Tran, and W. Choi, "Implementation of the constant current and constant voltage charge of inductive power transfer systems with the double-sided LCC compensation topology for electric vehicle battery charge applications," *IEEE Trans. Power Electron.*, vol. 33, no. 9, pp. 7398–7410, Sep. 2018.

[6] J. Lu, G. Zhu, D. Lin, Y. Zhang, J. Jiang, and C. C. Mi, "Unified load-independent ZPA analysis and design in CC and CV modes of higher order resonant circuits for WPT systems," *IEEE Trans. Transp. Electrific.*, vol. 5, no. 4, pp. 977–987, Dec. 2019.

[7] X. Qu, H. Han, S. C. Wong, C. K. Tse, and W. Chen, "Hybrid IPT topologies with constant current or constant voltage output for battery charging applications," *IEEE Trans. Power Electron.*, vol. 30, no. 11, pp. 6329–6337, Nov. 2015.

[8] R. Mai, Y. Chen, Y. Li, Y. Zhang, G. Cao, and Z. He, "Inductive power transfer for massive electric bicycles charging based on hybrid topology switching with a single inverter," *IEEE Trans. Power Electron.*, vol. 32, no. 8, pp. 5897–5906, Aug. 2017.

[9] X. Qu, Y. Jing, J. Lian, S. C. Wong, and C. K. Tse, "Design for continuous-current-mode operation of inductive-power-transfer converters with load-independent output," *IET Power Electron.*, vol. 12, no. 10, pp. 2458–2465, Oct. 2019.

[10] R. Bosshard, J. W. Kolar, J. Muhlethaler, I. Stevanovic, B. Wunsch, and F. Canales, "Modeling and η-α-Pareto optimization of inductive power transfer coils for electric vehicles," *IEEE J. Emerg. Sel. Top. Power Electron.*, vol. 3, no. 1, pp. 50–64, Mar. 2015.